Immunity, Vol. 3, 509–519, October, 1995, Copyright © 1995 by Cell Press

Anatomy of Autoantibody Production: Dominant Localization of Antibody-Producing Cells to T Cell Zones in Fas-Deficient Mice

Bruce A. Jacobson,* David J. Panka,*
Kim-Anh Nguyen,† Jan Erikson,†
Abul K. Abbas,‡ and Ann Marshak-Rothstein*
*Department of Microbiology
Boston University School of Medicine
Boston, Massachusetts 02118
†The Wistar Institute
3601 Spruce Street
Philadelphia, Pennsylvania 19104
‡Immunology Research Division
Department of Pathology
Brigham and Women's Hospital
Harvard Medical School
Boston, Massachusetts 02115

Summary

The goal of this study was to examine the in vivo site of autoantibody production in normal and autoimmune-prone mice. B cells were identified in tissue sections with IgM- and IgG2a-specific riboprobes that readily distinguished resting cells from antibody-forming cells (AFC). In normal mice, the few identifiable IgG2a-secreting cells were found in the red pulp. By contrast, in *lpr* mice exceedingly high numbers of IgG2a and autoantibody-producing cells were found deep within the T cell-rich periarteriolar lymphoid sheaths (PALS). This unusual anatomic location of autoantibody-secreting B cells is unique to Fas dysregulated strains, since IgG2a-producing cells in MRL/+ and (SWR × NZB)F1 mice were found predominantly in the red pulp or outer PALS, similar to normal mice. Furthermore, analysis of spleens from *lpr* and non-*lpr* anti-DNA immunoglobulin transgenic mice revealed dramatic accumulation of Tg^+ cells in the inner PALS only in *lpr* mice. These data suggest that in the absence of Fas, autoreactive B cells accumulate in T cell-rich zones, and this anatomic feature may contribute to autoantibody production.

Introduction

The homozygous recessive mutations, *lpr* and *gld*, have recently been mapped to the genes encoding the membrane proteins Fas and Fas ligand (FasL), respectively (Itoh et al., 1991; Watanabe-Fukunaga et al., 1992a; Adachi et al., 1993; Takahasi et al., 1994). This receptor–ligand combination is involved in the induction of apoptosis (Trauth et al., 1989; Yonehara et al., 1989: Itoh et al., 1991; Watanabe-Fukunaga et al., 1992b; Ju et al., 1995; Rothstein et al., 1995). Immunoregulatory defects resulting from the inability of lymphocytes to respond to Fas/FasL-mediated apoptotic signals lead to an early onset autoimmune syndrome associated with excessive autoantibody production (Cohen and Eisenberg, 1991). By 10 weeks of age, serum immunoglobulin G2a (IgG2a) titers are at least 10-fold higher in MRL/*lpr* mice than in MRL/+ mice, and anti-IgG2a rheumatoid factor (RF) titers are commonly 100-fold higher. With disease progression, serum IgG2a levels of MRL/*lpr* mice frequently increase to 20- to 50-fold above control values, while the RF titers can increase 10,000-fold (Wolfowicz et al., 1988). Monoclonal or oligoclonal expansions of RF-producing cells have been shown to contribute significantly to the serum RF titers (Shlomchik et al., 1987, Wolfowicz et al., 1988). Although it is not known what fraction of IgG2a-producing B cells is specific for autoantigens, anti-nuclear autoantibodies frequently use the IgG2a isotype (Slack et al., 1984; Rubin et al., 1986), and anti-DNA and anti-Sm antibodies have also been shown to undergo monoclonal or oligoclonal expansions (Eisenberg et al., 1982; Shlomchik et al., 1990; Bloom et al., 1993). Therefore, it is likely that autoantibodies of the IgG2a subtype contribute significantly to IgG2a serum levels.

Previous in vivo studies have demonstrated an intrinsic defect in *lpr* B cells. In various chimeric animal models where *lpr* B cells were allowed to develop in vivo alongside normal B cells, it was found that the vast majority of circulating IgM and IgG was derived from the *lpr* B cells (Perkins et al., 1990; Nemazee et al., 1991). In such chimeras, normal B cell development and function were presumably curtailed by FasL-dependent mechanisms. It was further shown that to develop autoantibody production, both the T and B cell compartments had to express the *lpr* defect (Sobel et al., 1991). These studies strongly indicated that the development of autoantibody production in *lpr* mice is not simply the result of excessive or abnormal T cell help. Subsequent in vitro experiments have shown that the *lpr* defect directly affects B cell regulation, resulting in an inability of B cells (Rothstein et al., 1995), as well as T cells (Ju et al., 1995; Brunner et al., 1995, Dhein et al., 1995), to undergo Fas-mediated apoptosis. Despite these documented effects of the *lpr* mutation on B cell survival and autoantibody production, conventional antibody responses in prediseased *lpr* mice, but not diseased animals, appear relatively normal (Creighton et al., 1979; Park et al., 1983; Very et al., 1993), suggesting a functional dichotomy between autoantibody and conventional antibody responses.

The inability of *lpr* B cells to undergo FasL-mediated apoptosis has been shown to lead to an apparent breakdown in peripheral B cell tolerance. Rathmell and Goodnow (1994) have examined the B cell compartments of normal and *lpr* mice expressing a combination of anti-hen egg lysozyme (HEL) B cell receptor transgenes and endogenous HEL. They found that elimination of HEL-reactive B cells exposed to membrane-bound HEL occurred comparably in *lpr* and normal mice, and concluded that defective Fas expression did not interfere with central B cell tolerance induction. However, in studies with soluble HEL transgenic (Tg) mice, they found that the maintenance of peripheral tolerance in the *lpr* anti-HEL mice was leakier

than in their non-*lpr* counterparts; a significant percentage of these older *lpr* double-transgenic animals developed elevated titers of serum anti-HEL antibody and had increased numbers of splenic anti-HEL antibody-forming cells (AFCs), indicating a breakdown in normal homeostatic control mechanisms.

In another transgenic model of B cell tolerance, Erikson et al. (1991) found that in non-*lpr* mice transgenic for an anti-ssDNA B cell receptor, $V_H3H9/V\kappa8$, the Tg^+ B cells persisted but their immunoglobulin was not present in the serum. Recent studies have shown that these B cells are functionally crippled (K.-A. N. and J. E., unpublished data). Similarly, Roark et al. (1995) found that in non-*lpr* mice transgenic for the anti-DNA-associated V_H3H9 IgH chain, B cells failed to produce detectable levels of antibodies with a homogeneous nuclear (HN) reactivity pattern; the corresponding MRL/*lpr* Tg mice had elevated serum titers of both anti-DNA- and anti-HN-staining autoantibodies. HN-specific autoantibodies are prevalent in patients with systemic lupus erythematosus (Wallach, 1992). These results further demonstrate that deficient Fas expression can result in defective regulation of autoreactive B cells.

To understand better the role of the *lpr* mutation in the breakdown of B cell tolerance and the production of autoantibodies, it was important to determine when and where in the course of B cell differentiation defective Fas expression could predispose an autoreactive B cell to actively produce autoantibodies. To address this issue, we investigated the anatomic localization of autoreactive B cells in the spleens of MRL/*lpr* mice, anticipating that their location might differ from that of antibody-secreting cells specific for conventional foreign antigens. It was reasoned that identification of the site where autoantibody producing cells accumulate might also elucidate how the *lpr* defect in B cells leads to autoantibody production and could identify the critical point in B cell development where Fas expression plays a role in maintaining tolerance.

We used in situ hybridization and immunohistochemistry to investigate the temporal and anatomic distribution of IgM- and IgG2a-producing B cells, as well as IgG2a-specific RF-producing cells, in splenic cryosections of *lpr* and non-*lpr* mice. Our results demonstrate that the inability to express Fas leads to an unusual and predominant localization of IgG2a AFC and anti-IgG2a RF-producing cells to the T cell–rich inner PALS. This distribution pattern was not apparent in either young (10 weeks) or old (7 months) MRL/+ spleen, or in the non-*lpr* (SWR × NZB)F1 (SNF1) autoimmune strain. Moreover, in an autoreactive immunoglobulin transgenic system, B cells developing in an *lpr* environment localized to the inner PALS, while B cells expressing the same receptor in a non-*lpr* environment did not. These results demonstrate that deficient Fas expression can lead to the accumulation of B cells in the T cell–rich inner PALS. Continuous exposure to autoantigen and T cell help in this locale may result in the uncontrolled activation of B cells and subsequent dysregulated production of autoantibodies.

Results

The Cμ and Cγ2a^J Digoxigenin-Labeled Riboprobes Specifically Detect IgM- and IgG2a-Expressing Cells

Prior to using the digoxigenin (DIG)-labeled IgM (Cμ) and IgG2a (Cγ2a^J) riboprobes on splenic tissue, we demonstrated their specificity on B cell hybridoma cytospin preparations. Figure 1 shows that the two antisense riboprobes, Cμ and Cγ2a^J, strongly label cells making IgM and IgG2a mRNA, respectively, and that they do not cross-hybridize. The Cμ probe specifically hybridized to an IgM-

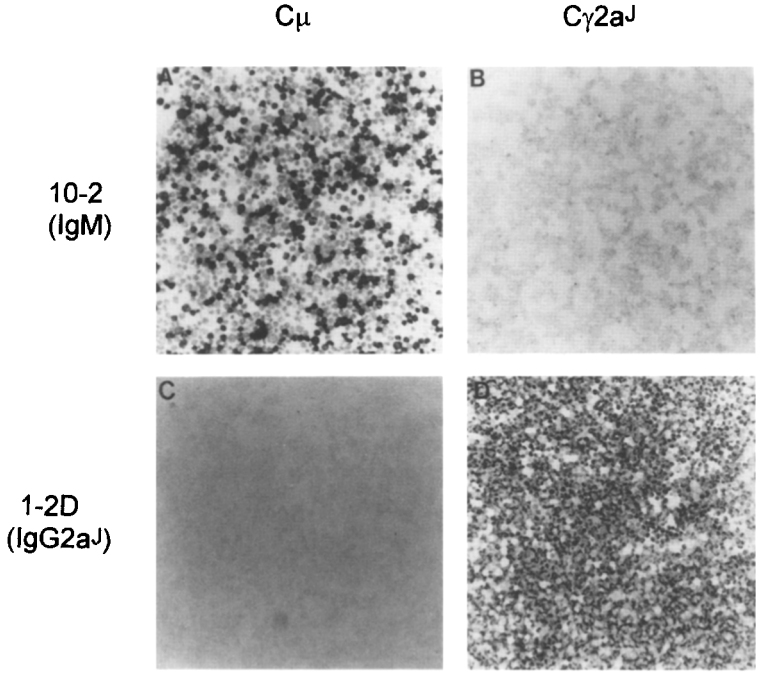

Figure 1. Specificity of Cμ and Cγ2a^J Anti-Sense Riboprobes

Cytospin preparations of MRL/lpr RF-producing hybridomas 10-2 (IgM) and 1-2D (IgG2a^J) were hybridized with IgM and IgG2a antisense riboprobes. The Cμ anti-sense DIG-labeled riboprobe hybridized to 10-2 cells (A) but not to 1-2D cells (C). The Cγ2a^J riboprobe did not hybridize to 10-2 cells (B) but did bind to 1-2D cells (D). The hybridized probes were detected with sheep anti-DIG–alkaline phosphatase and the substrates NBT and BCIP. Original magnification, 250×.

secreting hybridoma, 10-2, but not to an IgG2a-secreting hybridoma, 1-2D, while the Cγ2a^J probe exhibited the reciprocal specificity. The Cμ and Cγ2a^J riboprobes also failed to cross-react with IgG1-, IgG2b-, IgG3-, and IgA-producing cell lines (data not shown). Additionally, the Cγ2a^J sense riboprobe did not hybridize to splenic tissue from MRL/lpr mice positive for IgG2a-producing cells (data not shown).

Anatomic Location of Resting and Activated B Cells

When hybridized to splenic cryosections, the anti-sense Cμ riboprobe readily distinguished the lightly staining resting sIgM$^+$ B cells from the more darkly staining AFC. The resting B cells in normal mice were mainly found in the outer PALS region of the white pulp, surrounding the CD4$^+$ and CD8$^+$ T cells present in the inner PALS (Figures 2A and 2B). A similar distribution was found in young MRL/*lpr* mice. By comparison, the IgM AFCs in normal mice were localized predominantly in the red pulp, in many cases associated with the terminal arterioles, or with marginal zone–bridging channels that traverse the marginal zones into the red pulp (Mitchell, 1973). IgM AFCs present in both young and old MRL/+ mice (11–32 weeks of age) showed a similar red pulp distribution (data not shown). Only rarely were IgM AFCs found in the inner PALS.

While prediseased MRL/*lpr* mice resembled the MRL/+ pattern, by 10–12 weeks of age, the IgM AFCs in the MRL/*lpr* spleen exhibited a more heterogeneous distribution pattern. Many IgM AFCs were identified in the B cell outer PALS, in the red pulp, and along the terminal arterioles. Most significantly, unexpectedly high numbers of IgM AFCs were found in the T cell–rich inner PALS. Within a particular section, variation existed among the apparently anatomically distinct T cell regions in that certain PALS appeared to have a higher concentration of IgM AFCs than others (Figures 2D and 2E).

IgG2a-Producing B Cells Exhibit a Predominant Localization to the Inner PALS in MRL/*lpr* Spleen

The Cγ2a^J probe detected very few resting B cells or AFCs in sections from normal BALB/c or MRL/+ spleen (Figure 2C). As expected, those few IgG2a AFCs were located

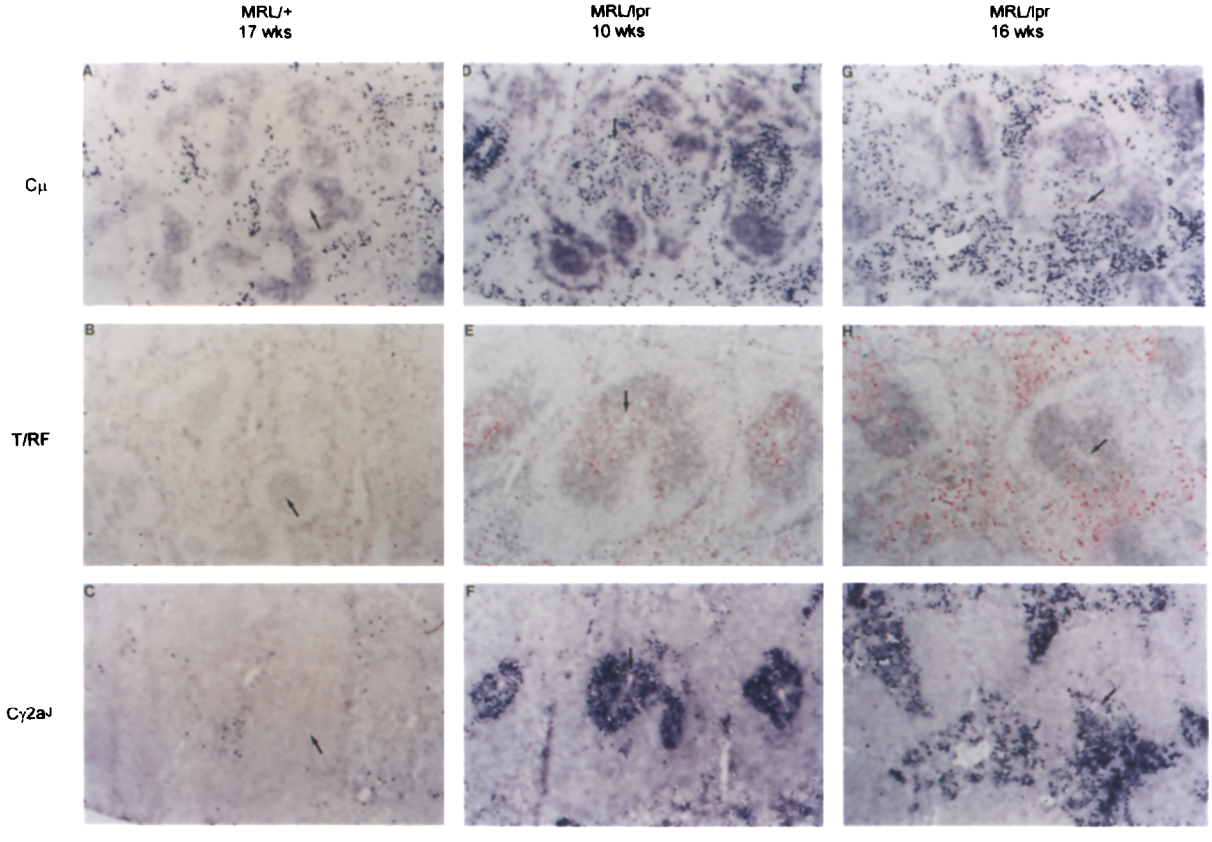

Figure 2. In Situ Localization of IgM-, IgG2a-, and RF-Producing Cells in Young and Old *lpr* and Normal Murine Splenic Tissue Sections

IgM- and IgG2a-expressing cells were detected by in situ hybridization and T cells and RF-producing cells were identified by immunohistochemistry. Serial 6 μm splenic tissue sections were hybridized with either the anti-sense DIG-labeled riboprobes Cμ (A, D, and G) or Cγ2a^J (C, F, and I), and detected with sheep anti-DIG–alkaline phosphatase and NBT/BCIP. NBT/BCIP produces a blue/black precipitate. Resting IgM$^+$ cells exhibit a faint dark stain, whereas IgM- and IgG2a-producing cells appear more darkly stained. Sections were also double-stained with anti-CD4DIG, and anti-CD8DIG, and 23BIO to identify T cells and RF-producing cells, respectively (B, E, and H). DIG-labeled antibodies were detected with sheep anti-DIG (gold) followed by silver enhancement, producing a brown precipitate. Localization of anti-IgG2a-binding RF B cells was demonstrated using the BIO-labeled reagent MAb 23 (IgG2a), followed by an avidin–biotin–alkaline phosphatase conjugate (ABC–AP) and the substrate Vector red. AP in the presence of Vector red produces a red precipitate. Arrows denote central arterioles in contiguous sections. Original magnification, 40×.

in the red pulp, often around the terminal arterioles. A dramatically different staining pattern was apparent in the 10- 12-week-old MRL/*lpr* spleens, where a dense accumulation of IgG2a AFCs was found interspersed with the single-positive (SP) T cells of the inner PALS, as identified by the staining of contiguous serial sections with CD4- and CD8-specific monoclonal antibodies (MAbs) (Figures 2E and 2F). Few IgG2a-producing cells were observed outside of the PALS. The accumulation of these IgG2a AFCs correlated with the onset of elevated serum IgG2a titers (data not shown). The close association between IgG2a AFC and SP $CD4^+/CD8^+$ T cells was less apparent with disease progression in the older (>16 weeks) MRL/*lpr* mice, as clusters of IgG2a AFCs appeared to shift from a predominant localization in the inner PALS to a more heterogeneous distribution pattern (Figures 2H and 2I). Similarly, the IgM AFCs in the older MRL/*lpr* became more heterogeneously dispersed (Figure 2G).

IgG2a-Specific RF-Producing B Cells Also Localize to the Inner PALS in MRL/*lpr* Mice

The majority of MRL/*lpr* mice develop extremely elevated anti-IgG2a RF titers, in part owing to extensive clonal expansions (Shlomchik et al., 1987). Therefore, the RF-secreting cells represent a prototypic autoantibody response. We developed an immunohistochemical staining technique that could specifically identify IgG2a-reactive RF-producing cells, using aggregated IgG2a as the detection reagent. To avoid nonspecific reactivity with Fc receptors, staining was routinely carried out in the presence of 4% normal rabbit serum (NRS). Under these conditions, the label reacted with RF-producing hybridoma cell lines, but not the SP2/0 fusion partner or the P388D1 macrophage-like cell line that expresses high affinity Fcγ2a receptors (Unkeless and Eisen, 1975) (data not shown).

Using biotinylated IgG2a (MAb 23) in tandem with DIG-tagged anti-CD4 and anti-CD8, we were able to demonstrate clearly that in 10- to 12-week-old MRL/*lpr* sections, large numbers of RF AFCs were predominantly localized to the T cell–rich inner PALS (Figure 2E), similar to the pattern observed with the $C\gamma2a^J$ probe. Although a few RF were found in the red pulp, the majority of RF-producing cells were restricted to the inner PALS. These sections demonstrate that autoantibody production in MRL/*lpr* mice occurs outside the anatomical environment normally associated with AFC. By comparison, very few anti-IgG2a RF-producing cells were detectable in the 17-week-old MRL/+ spleen, and those RF were mostly found in the red pulp (Figure 2B).

The striking PALS association of RF-producing cells seen in MRL/lpr mice early in disease also became more variable with disease progression (Figure 3D). By 16 weeks, as the splenic architecture deteriorated, clusters of RF AFCs appeared to shift into the red pulp (Figure 2H). At all timepoints, there was consistent colocalization of IgG2a AFCs and anti-IgG2a RF B cells in the MRL/*lpr* sections. It should be noted, however, that RF-expressing cells were observed in other locations in MRL/*lpr* spleen at 10–16 weeks: they were observed near the terminal arterioles in the red pulp, and as clumps of cells at the outer edge of the T cell zone, apposed to T cells. The clumps of RF-expressing cells at the interface of the outer and inner PALS are reminiscent of the foci described by Jacob et al. (1991a).

Double-Negative T Cells Do Not Colocalize with AFC in *lpr* Mice

Double-negative (DN) T cells accumulate in the peripheral lymphoid tissues of *lpr* mice as disease progresses and are a major factor associated with the ensuing lymphoid hyperplasia (Morse et al., 1982; Theofilopoulos et al., 1985). Although these cells are relatively refractory to stimulation (Davignon et al., 1985), they have been shown to have cytotoxic activity (Budd et al., 1986), to produce cytotoxic molecules (Hammond et al., 1993), and even to secrete a factor that putatively promotes the differentiation of resting B cells (Prud'homme et al., 1983). The DN T cells could be identified in splenic cryosections with a combination of MAbs specific for B220 and mouse κ light chain. Since both the DN T cells and B cells express B220, but only the B cells express κ light chain, the DN T cells appeared red and the B cells appeared brownish-red with this staining protocol. As expected, DN T cells could not be detected in MRL/+ spleen, and only B cells were evident in the regions surrounding the SP T cells in the inner PALS (Figures 3A and 3B). However, by 10–12 weeks of age, many DN T cells were detectable in the MRL/*lpr* spleen. They were found in the B cell–rich outer PALS, surrounding $CD4^+$ and $CD8^+$ T cells in the inner PALS, and their numbers increased with disease progression. In the later stages of disease, DN T cells occupy most of the outer PALS, to the exclusion of resting $sIgM^+$ B cells (Figures 3C and 3D). At all times, the localization of the DN T cells to the resting B cell compartment of the outer PALS, also noted by Lieberum and Hartmann (1988), was clearly distinct from the localization of AFCs in the T cell–rich inner PALS. The anatomic segregation of AFCs and DN T cells indicates that these T cells are probably not directly involved in B cell activation.

Localization of IgM and IgG2a AFC in Other Autoimmune Strains

It was important to determine whether the abnormal localization of IgM and IgG2a AFCs to the inner PALS in the MRL/*lpr* spleen was a general phenomenon characteristic of all autoantibody responses or whether it was unique to the *lpr* mutation. Two approaches were taken to address this issue. First, we examined splenic sections from SNF1 mice, another autoimmune strain known to develop high titers of IgG2a and autoantibodies. IgM and IgG2a AFCs were not found in the inner PALS of young (4 weeks) or older (25 weeks) SNF1 mice (Figures 4A–4F), indicating that the inner PALS localization of AFCs seen in *lpr* mice was not characteristic of all autoantibody-producing cells. IgG2a AFCs in the 25-week-old SNF1 mice were present in clusters in the outer PALS and dispersed throughout the red pulp.

The second approach involved the examination of splenic sections from mice expressing an autoreactive transgenic B cell receptor. The transgenic receptor $V_H3H9/$

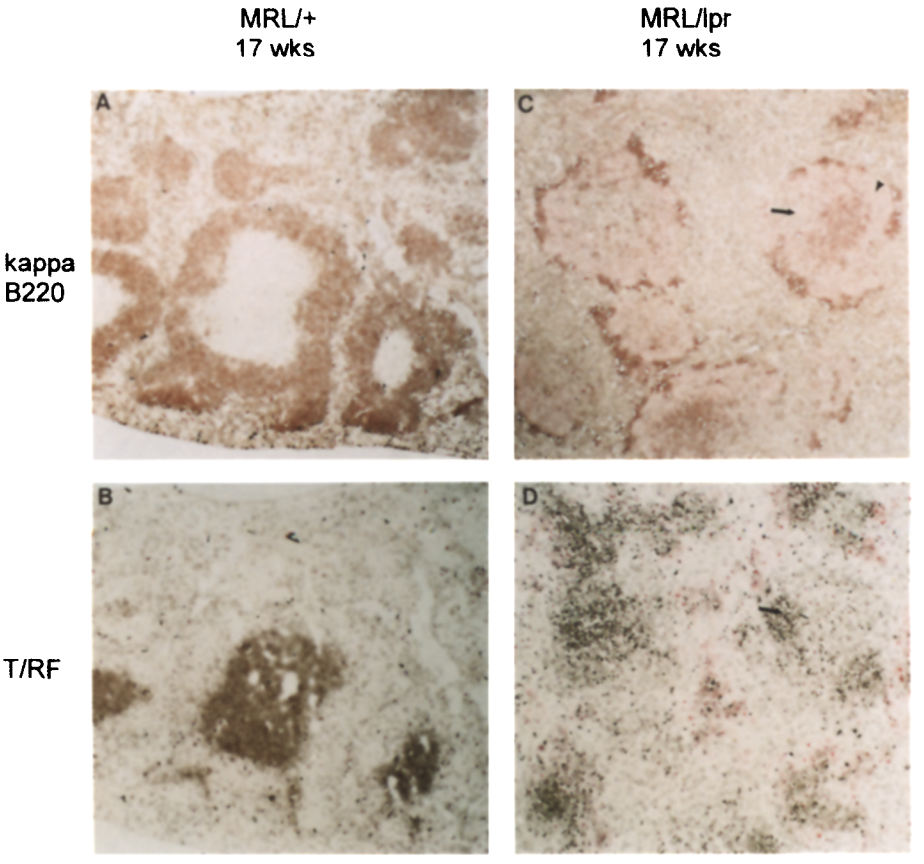

Figure 3. Accumulation of B220⁺ DN T Cells in the Spleen, in the B Cell Region of the White Pulp

Tissue sections from 17-week-old MRL/+ (A) and MRL/*lpr* (C) mice were stained with anti-κ DIG and B220BIO to distinguish the B220⁺ DN T cells from the B220⁺ κ⁺ B cells. The anti-κ DIG was developed with sheep anti-DIG (gold), followed by silver enhancement, producing a brown precipitate. B220BIO staining was followed by addition of avidin–biotin–alkaline phosphatase conjugate (ABC–AP) and the substrate Vector red. AP in the presence of Vector red produces a red precipitate. The double staining of resting B cells with anti-κ DIG and B220BIO produced a brownish-red stain. Antibody-producing κ⁺ cells do not express B220 and therefore appear brown. DN T cells do not express κ and therefore appear red, and are localized to the region between the inner PALS T cells and the marginal zone B cells. Serial sections of the MRL/+ and MRL/lpr spleen, respectively, were stained with reagents to identify T cells and RF-producing cells, as in Figure 2(B and D). A site of DN T cell accumulation is designated by an arrowhead, and a T cell–rich inner PALS is denoted with arrows in an MRL/*lpr* spleen (C and D). Original magnification, 40×.

Vκ8 has been shown to bind ssDNA (Radic et al., 1991). Expression of this receptor in non-*lpr* mice does not lead to detectable levels of circulating DNA-specific antibodies, although Tg⁺ B cells are known to constitute a major proportion of the splenic B cell population (Erikson et al., 1991). Examination of sections from these non-*lpr* Tg⁺ mice revealed a relatively normal distribution of resting sIgM⁺ B cells or IgM⁺ AFC (Figures 5A and 5B). However, a direct comparison of Tg⁺ and Tg⁻ sections suggested that a limited (but significantly different from control) number of Tg⁺ cells were present in the inner PALS.

A very different staining pattern was apparent in the V_H3H9/Vκ8 *lpr* mice. As shown in Figures 5D and 5E, staining of contiguous sections with the Cμ riboprobe and anti-CD4 and anti-CD8 MAbs identified clusters of IgM AFCs in the T cell–rich inner PALS of 8-week-old Tg⁺ MRL/*lpr* mice. Non-Tg *lpr* littermates had typical clusters of inner PALS–associated IgG2a AFCs (Figure 5I) that were not present in either the Tg⁺ BALB/c or Tg⁺ MRL/*lpr* mice (Figures 5C and 5F), presumably owing to constraints of the IgM construct. Altogether, these data strongly indicate that the association of autoreactive B cells with the inner PALS is unique to mice expressing defects in Fas/FasL-mediated regulation.

Discussion

The *lpr* mutation in MRL mice profoundly affects the regulation of both T and B lymphocytes, leading to the excessive production of autoantibodies. To understand better the role of Fas/FasL-mediated apoptosis in the control of autoreactive B cells, we felt it was important to identify the specific localization of autoantibody-producing cells in Fas-deficient mice. Our observations indicate that the *lpr* defect leads to a dramatic localization and accumulation of antibody-forming cells in the inner PALS of the spleen, a site from which they are normally excluded.

For the purposes of this study, we chose to examine four types of B cells: resting sIgM⁺ B cells, IgM-secreting B cells, IgG2a-secreting B cells, and anti-IgG2a RF-secreting B cells. Resting sIgM⁺ B cells are the dominant B cell population in normal lymphoid tissues, and their

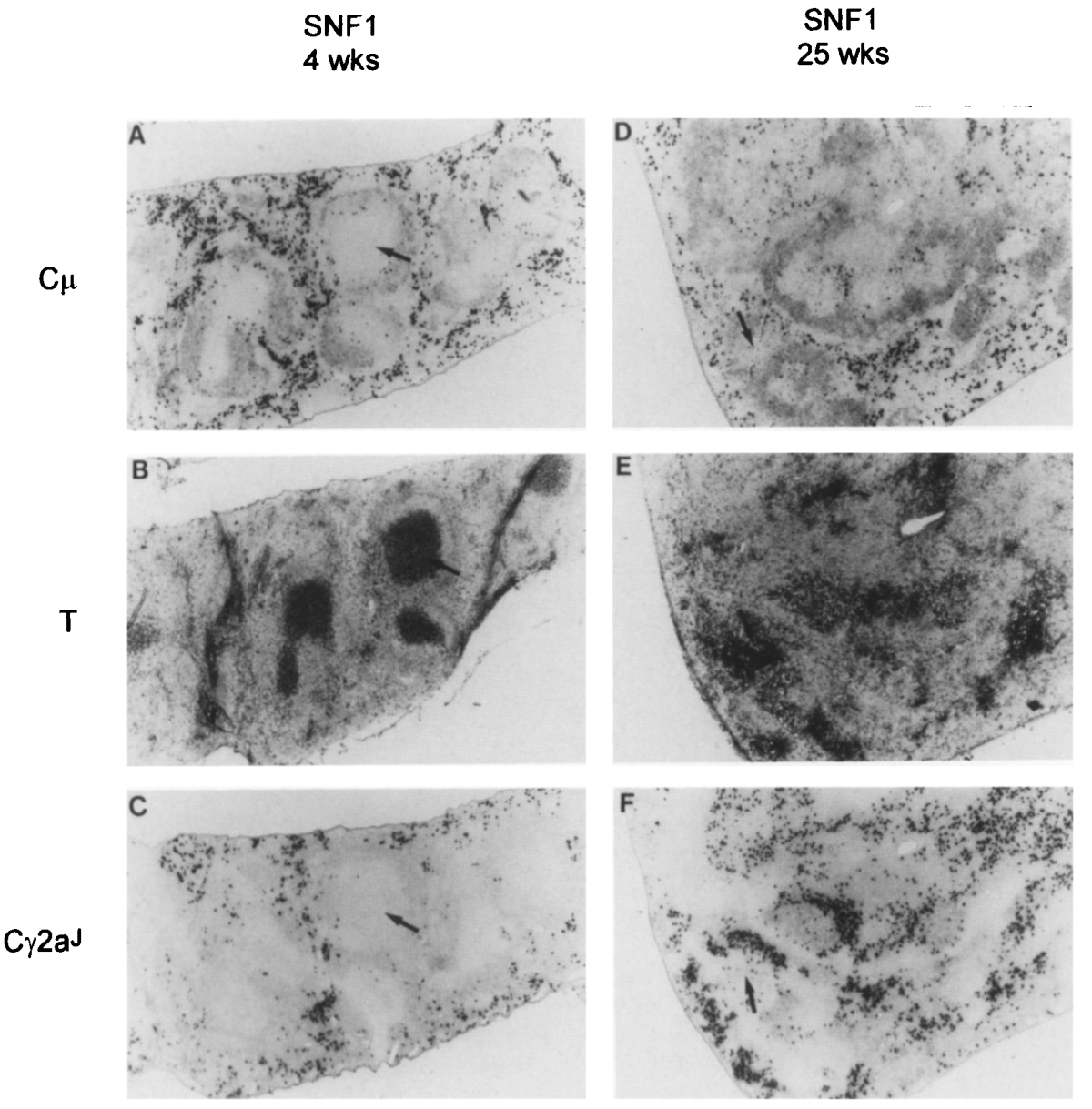

Figure 4. Localization of IgG2a AFC in SNF1 Mice

Splenic cryosections from young (4 weeks) or old (25 weeks) SNF1 mice were hybridized with either the anti-sense DIG-labeled riboprobes Cμ (A and D), or Cγ2a^J (C and F) to detect IgM- and IgG2a-expressing cells, respectively, as described in Figure 2, or with anti-CD4DIG and anti-CD8DIG (B and E). CD4$^+$ and CD8$^+$ SP T cells were visualized with sheep anti-DIG (gold) and silver enhancement. Arrows denote central arterioles in contiguous tissue sections. Original magnification, 132×.

location provides an anatomic landmark by which to locate spatially the other responding cell types. In contrast, B cells actively secreting IgM are less prevalent in normal mice but have been associated with the early stages of *lpr* disease (Klinman, 1990). The use of a Cμ riboprobe to identify IgM$^+$ B cells had a major advantage over the use of conventional anti-IgM antibody reagents in that it clearly distinguished resting IgM$^+$ B cells from IgM AFCs on the basis of hybridization intensity. T cell areas surrounding the central arterioles could be clearly delineated by the absence of Cμ riboprobe staining, and by the presence of CD4$^+$ and CD8$^+$ T cells using the appropriate immunohistochemical stains on contiguous serial tissue sections.

IgG2a-producing B cells were important to this analysis for several reasons. The appearance of high titers of IgG2a antibodies in the serum of diseased MRL/*lpr* mice correlates with the progression of disease, and a major proportion of the disease-associated anti-nuclear autoantibodies are of this isotype (Slack et al., 1984; Rubin et al., 1986). Furthermore, IgG2a (as opposed to IgM) antibody expression typically requires T cell help, and we wanted to include potentially T cell–dependent (TD) autoantibodies in our analysis. A Cγ2a^J riboprobe was used to identify IgG2a-

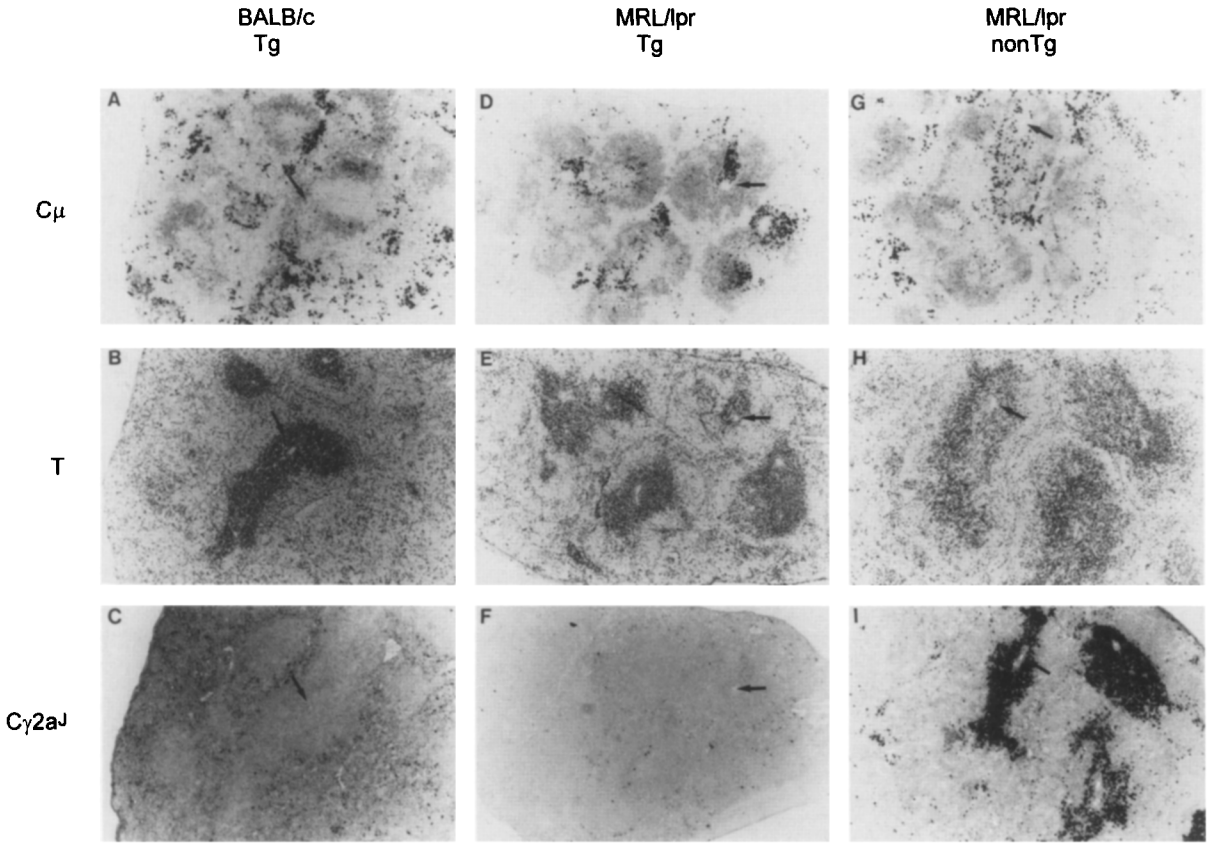

Figure 5. Distribution of IgM-Expressing Anti-DNA Transgenic B Cells in Normal and *lpr* Spleens

Splenic cryosections from V_H3H9/Vκ8 Tg BALB/c, Tg MRL/*lpr*, and non-Tg MRL/*lpr* mice were hybridized with either the anti-sense DIG-labeled riboprobes Cμ (A, D, and G), or Cγ2a^J (C, F, and I), or anti-CD4DIG and anti-CD8DIG (B, E, and H) as described in Figure 2. Arrows denote central arterioles in contiguous tissue sections. Original magnification, 132×.

producing cells. In this case, the use of in situ hybridization was essential for identification of cells producing IgG2a; conventional anti-IgG2a immunohistochemistry, based on the use of IgG2a-specific antibodies, was not informative because it could not differentiate cells making the IgG2a from the IgG2a in the interstitial spaces or bound to cell surfaces.

Anti-IgG2a RF-producing B cells were included as a prototypic autoantibody specificity. RF are a dominant component of the autoantibody pool of MRL/*lpr* mice. Elevated RF titers are found in most MRL/*lpr* mice, usually by 10 weeks of age, and 10%–20% of the hybridoma cell lines isolated from diseased *lpr* mice have been found to have RF activity (Wolfowicz et al., 1988). It is assumed that RF B cells receive T cell help as part of their maturation process, since they have been shown to undergo extensive clonal expansion and somatic mutation (Shlomchik et al., 1987).

The DN T cell subset represents a major cell type in the peripheral lymphoid compartments of diseased *lpr* mice. Our studies demonstrated that the DN T cells did not colocalize with the AFC, consistent with recent in vitro studies showing that DN T cell populations rigorously depleted of SP T cells are functionally inert and incapable of providing B cell help (A. K. A. and A. M.-R., unpublished data). Their progressive accumulation in the white pulp of the spleen disrupts the anatomic organization and compartmentalization of the various cell populations. The distortion of the splenic architecture likely affects the ability of both T cells and B cells to collaborate efficiently to mount a humoral response to a conventional foreign antigen. We monitored the kinetics of the accumulation of DN T cells relative to the time at which AFCs begin to localize to the inner PALS, to assess whether the AFC–PALS association was a secondary effect tied to disruption of the splenic architecture. This does not appear to be the case, as significant accumulation of AFCs to the inner PALS was noted in mice with minimal numbers of DN T cells. Futhermore, Mountz et al. (1987) has shown that cyclosporin A treatment of MRL/lpr mice inhibited the expansion of the DN T cells, yet did not affect serum autoantibody or immunoglobulin titers. This issue can be further evaluated in anti-CD8-treated (Giese and Davidson, 1994) or major histocompatibility complex class I knockout *lpr* mice (Mixter et al., 1995; Giese and Davidson, 1995), since these mice still make autoantibodies but do not develop DN T cells or lymphadenapathy.

Recent studies have begun to elucidate the dynamics and anatomy of antigen-specific B cell activation and AFC formation, and it was important to examine the anatomic

localization of autoantibody production in the context of these reports. The anatomic site for antigen-specific B cell differentiation to antibody-producing cells has been identified by the use of immunohistochemical techniques on splenic cryosections. B cells follow two distinct pathways of antigen-induced activation: an extrafollicular pathway of antibody secretion and heavy chain isotype switching, and an intrafollicular (germinal center) pathway of somatic hypermutation, affinity maturation, and memory cell generation (McHeyzer-Williams et al., 1993). The first AFCs to develop during an immune response were observed by Van Ewijk et al. (1977) to occur at the border of the T and B cell domains in the PALS. It appears that after a primary immunization with either TD or T cell–independent (TI) antigens, most antigen-specific AFCs are localized to the outer PALS and the sheaths of lymphoid tissue surrounding the terminal arterioles (Van Rooijen et al., 1986; MacLennan et al., 1990; Liu et al., 1991; Van Eertwegh et al., 1993). Additionally, Van Rooijen et al. (1986) found that AFCs that arose during a secondary response were found in the same anatomic sites within the spleen. Kelsoe and colleagues (Jacob et al., 1991a) have further analyzed the anatomic location of the first AFCs to appear shortly after immunization. They showed that 2 days after immunization of C57BL/6 mice with a hapten–protein conjugate, low numbers of B cells making detectable amounts of hapten-specific antibody were located at the periphery of the PALS and around the terminal arterioles. By day 6 postantigen challenge, the antigen-specific AFCs had condensed to form foci, in apposition to T cells at the junction of the inner and outer PALS. Thus, according to our current understanding, it appears that early in a primary response antigen-specific antibody-producing B cells arise at the interface of the inner and outer PALS and then can be seen migrating out of the white pulp along the marginal zone–bridging channels. Other sites of AFC localization have not previously been described.

The surprising observation of inner PALS localization of IgG2a AFCs in MRL/*lpr* mice contrasts dramatically with the observed localization of IgG2a AFCs to the outer PALS, red pulp, and the sheaths of the terminal arterioles in normal BALB/c and MRL/+ as well as autoimmune SNF1 mice. We also found an *lpr*-associated dominant localization of cells secreting a prototypic autoantibody, anti-IgG2a RF, to the inner PALS of MRL/lpr mice. Furthermore, clusters of B cells expressing the V_H3H9/Vκ8 Tg B cell receptor were also found in the inner PALS of transgene-expressing *lpr* mice, although this accumulation was less striking than that observed in MRL/lpr mice. We have not analyzed *lpr* strains other than MRL, and have not studied lymph nodes or other tissues. However, the results with the immunoglobulin transgenic mice strongly supports the hypothesis that the abnormal accumulation of AFCs is associated with deficient Fas expression. Two examples of autoreactive B cell accumulation in the inner PALS have been reported by Goodnow and colleagues. In the first study, Cyster et al. (1994), using the double-transgenic soluble HEL/anti-HEL system, observed an accumulation of autoreactive B cells in the periphery of the inner PALS. When they reconstituted a lethally irradiated HEL Tg recipient with a mixture of anti-HEL Tg and normal non-Tg bone marrow cells, the anti-HEL autoreactive B cells were detained within the inner PALS, and thereby excluded from the microenvironment of mature recirculating B cells. The authors suggested that the detention and eventual death of the anti-HEL autoreactive B cells represented a unique pathway for the maintenance of tolerance. Thus, autoreactive anergic B cells, through a yet unknown mechanism, are unable to enter the B cell follicles and gain access to the mature recirculating pool of B lymphocytes.

In the second study, Shokat and Goodnow (1995), again using the anti-HEL Tg B cell system, noted that a subset of Tg^+ germinal center B cells that had been primed with duck egg lysozyme (DEL), for which their anti-HEL transgene has a 1000-fold lower affinity, migrated to the periphery of the inner PALS within 4 hr of being immunized with soluble HEL. They also found increased apoptosis in the T cell zone 4 hr after soluble HEL administration; however, if the Tg^+ B cells expressed a *bcl-2* transgene the cells survived in the inner PALS. These two reports demonstrate the phenomenon of B cell accumulation to the inner PALS and show that they are eliminated there unless they receive the appropriate survival signals. In contrast, we have observed a dense accumulation of IgG2a B cells to the central zone of the inner PALS in the MRL/*lpr* mouse. Not only do these B cells persist in the T cell zone, but they have been activated as indicated by their level of IgG2a mRNA.

Anergic B cells, under normal circumstances, appear to be excellent targets for FasL-mediated cytotoxicity (Rathmell et al., 1995). Sensitivity to FasL presumably results from activation through CD40 by a CD40L-expressing T cell in the absence of an effective protective signal delivered through the antigen-specific sIgM receptor (Rothstein et al., 1995). Since anergic *lpr* B cells are defective in Fas expression, they cannot be eliminated appropriately by Fas-dependent mechanisms. We propose that anergic autoreactive *lpr* B cells that have been retained in the inner PALS can be activated by helper T cells expressing CD40L. Such autoreactive B cells normally would be eliminated by means of the FasL coexpressed by the same activated T cell population. However, *lpr* B cells are resistant to such control signals, receive only positive signals from the neighboring activated T cells, and differentiate to autoantibody-secreting B cells. The architecture of the spleen, specifically the compartments of T cells in the inner PALS, recirculating IgM^+ B cells in the outer PALS, as well as the trafficking pattern of the various cell populations, likely provides not only an essential milieu for the efficient interaction of the appropriate cells for a humoral response (Van den Eertwegh et al., 1992), but also an efficient mechanism for the maintenance of B cell tolerance. Immunization of normal mice with potent immunogens does not lead to accumulation of AFCs in the inner PALS. This is not surprising, because we would predict that in conventional immune responses Fas–FasL interactions would continue to play their regulatory role.

It will be important to characterize further the clonality

and specificities of the inner PALS-associated AFCs, given that this appears to be the region where tolerance is broken in the Fas-deficient animal. Previous work from this lab has shown that *lpr* mice frequently exhibit clonal expansions of autoreactive B cells, particularly anti-DNA and RF. Additionally, these clones have been shown to undergo extensive somatic hypermutation. Together with the observations of the current report, these studies raise a number of provocative questions pertaining to the actual site of clonal expansion and somatic mutation in the *lpr* and *gld* models. Although numerous studies indicate the germinal centers are the major site of somatic mutation (Berek et al., 1991; Jacob et al., 1991b; McHeyzer-Williams et al., 1993) there is evidence that somatic mutation is not always restricted to the germinal centers (Chu et al., 1995). Since B cells in mice that inherit the *lpr* defect do not undergo Fas-mediated apoptosis, we propose that Fas/FasL-associated mechanisms are responsible for the demise of autoreactive B cells that normally accumulate in the inner PALS; the persistence of these B cells in a milieu of autoreactive T cells, as may occur in Fas-deficient mice, eventually results in expansion, activation, and excessive autoantibody production.

Experimental Procedures

Animals

MRL MpJ-+/+ and MRL MpJ-*lpr/lpr* mice were purchased from Jackson Laboratory (Bar Harbor, Maine) and then maintained and bred at Boston University Medical Center Animal Care Facility under standard conditions. (SWR × NZB)F1 mice were provided by S. Datta (Northwestern University, Chicago, Illinois). The V_H3H9/Vκ8 Tg mice were bred and maintained in the core facility at the Wistar Institute. The heavy and light chain transgenes had been backcrossed for at least 11 generations onto both BALB/c and MRL-*lpr/lpr* genetic backgrounds by breeding with parental strains obtained from the Jackson Laboratory. Progeny of transgenic breedings were genotyped by polymerase chain reaction (PCR) amplification of tail DNA using transgene-specific primers, as described (Erikson et al., 1991). All V_H3H9/Vκ8 Tg mice were maintained as hemizygotes under specific pathogen-free conditions. For this study, we analyzed eight MRL/lpr homozygotes (6–25 weeks old) and three MRL/+ mice (6–30 weeks old), four anti-DNA immunoglobulin transgenics (2 +/+ and 2 *lpr/lpr*), and two (SWR × NZB)F1 mice.

Antibodies

MAbs used in this study, rat anti-mouse κ (RαMκ)(33-18); anti-CD4 (GK1.5); anti-CD8 (53-6.7); anti-B220 (6B2); IgG2a, λ, anti-NIP (23), were either conjugated to biotin (BIO) (Heitzman et al., 1974; Goding, 1976) or digoxigenin (DIG), according to the instructions of the manufacturer (Boehringer Mannheim, Indiannapolis, Indiana), and used for immunohistochemistry. For detection of RF-producing B cells, 23BIO (Igh-1^J) was heat-aggregated immediately before use by diluting to 500 μg/ml in phosphate-buffered saline (PBS) and heating at 63°C for 30 min (Jacobson et al., 1994).

Immunohistochemistry

Murine spleens were snap-frozen in OCT (Tissue-Tek, Elkhart, Indiana) by submersing in 2-methylbutane cooled by liquid nitrogen for 4–5 s. Longitudinal sections 6 μm thick were thaw mounted onto Biobond (Biocell, Cardiff) coated glass slides, quickly fixed by dipping in ice-cold acetone for 4–5 s, and stored at −20°C until ready to use. For all immunohistochemical staining, previously cut cryosections were transferred quickly to ice-cold acetone, fixed for 3 min, washed three times for 5 min in PBS, and preincubated with 4% NRS. Biotin-labeled antibody solutions containing 4% NRS were added to the sections and incubated for 60 min in a humidified chamber. The biotin-stained slides were washed three times in PBS, incubated for 60 min with an avidin–biotin–alkaline phosphatase conjugate (ABC-AP, Vector Labs, Burlingame, California), washed again as above, and incubated with Vector red substrate solution (Vector Labs) containing 1 mM levamisole. All tissues stained with DIG-labeled antibodies were preincubated as above with 4% NRS, followed by incubation with the DIG-labeled antibodies for 60 min. The sections were then washed three times in PBS and incubated with 5% nonfat dry milk in PBS containing 4% NRS, washed again, and incubated with 100 μl sheep anti-DIG gold (5 nm) (Goldmark Biologicals, Phillipsburg, New Jersey) diluted 1:100 in PBS, 4% NRS for 60 min. The slides were then washed three times in 0.05 M sodium citrate, and 100 μl of silver enhancement solution added (Biocell). The gold bound to the tissue reduced the silver in solution and a brown/black deposit developed. For double-staining with BIO- and DIG-coupled antibodies, tissue sections were blocked as above, and then both primary antibodies were added simultaneously. When sections were stained with 23BIO, the incubation was done overnight at 4°C. After incubation with the primary reagents, the sections were rinsed three times in PBS and incubated with 5% nonfat dry milk containing 4% NRS, rinsed in PBS, and incubated with a 1:100 dilution of sheep-anti-DIG gold (5 nm) for 60 min. After the sheep-anti-DIG gold (5 nm) was removed, the sections were incubated with ABC-AP for another 60 min, washed three times in 50 mM sodium citrate, and then incubated with silver enhancement solution until adequate color development. The sections were rinsed twice in 50 mM sodium citrate, followed by a rinse in PBS. They were then incubated with the Vector red substrate solution.

Riboprobes

Two RNA probes were used for in situ hybridization, Cμ, and Cγ2a^J. The Cμ probe was provided by R. P. Bucy (University of Alabama, Birmingham, Alabama). The Cμ plasmid contained an 800 bp EcoRI–HindIII fragment from the mouse heavy chain IgM constant region. The fragment included bases 283–1084. The constant region fragment contained a BamHI site at nucleotide postition 578 downstream of the SP6 RNA polymerase transcription start site. The plasmid was linearized with BamHI and transcribed with SP6 RNA polymerase and deoxynucleotides containing dUTP-DIG (according to the manufacturer, Boehringer-Mannheim), to give DIG-labeled anti-sense transcripts of approximately 570 bases. DIG-labeled sense transcripts of approximately 800 bases were produced by linearizing Cμ with HindIII and transcribing with T7 RNA polymerase. The Cγ2a^J probe was constructed in this laboratory. The Cγ2a^J insert was derived from PCR-amplified DNA from the CH3 region (base pairs 1053–1325) of hybridoma 23 cDNA. The insert was cloned into pGEM1. Anti-sense DIG-labeled IgG2a transcripts of approximately 280 bases were produced by linearizing the plasmid with EcoRI and transcribing with SP6 RNA polymerase. DIG-labeled sense transcripts of 280 bases were produced by linearizing the plasmid with HindIII and transcribing with T7 RNA polymerase. DIG-labeled riboprobes were produced according to the instructions of the manufacturer (Boehringer-Mannheim, Indiannapolis, Indiana).

In Situ Hybridization

Tissue sections 6 μm thick were cut in a cryostat with an RNase-free cryostat blade and thaw mounted onto cleaned and baked RNase-free glass slides. The sections were air dried for 10–20 min at room temperature, and then fixed in 3% paraformaldehyde in PBS for 1 hr. The slides were rinsed in 0.1 M triethanolamine (Sigma) (pH 8.0) for 5 min, and then the tissue was acetylated by incubation in 0.1 M triethanolamine, with 0.25% acetic anhydride (Sigma), for 15 min, and rinsed again in 0.1 M triethanolamine. The sections were incubated with prehybridization solution (50% formamide, 4× SSC, 250 μg/ml of yeast tRNA, 0.4× Denhardt's, 10% dextran sulfate, and 500 μg/ml salmon testes DNA; the DNA was heated to 65°C for 10 min prior to use) for 1 hr. DIG-labeled riboprobe (10 μl) (denatured by heating to 80°C for 5 min) was added to the underside of a siliconized coverslip, applied to the section, sealed with nail polish, and hybridized at 52°C for 15–18 hr. Typically, 2–20 ng of Cμ probe and 1–2 ng of Cγ2a^J probe were used per slide. Following hybridization, the coverslips were removed and the slides rinsed three times in 2× SSC, followed by a rinse in STE (500 mM NaCl, 1 mM EDTA [pH 8.0], 20 mM Tris–HCl [pH 7.5]), and then incubated with RNase A (50 μg/ml) in STE at 37°C for 45 min. The slides were then incubated in 50% formamide, 2×

SSC at 53°C for 20 min, rinsed one time in 1× SSC, rinsed three times in 0.5× SSC, and finally rinsed one time in buffer #1 (100 mM Tris–Cl [pH 7.5], 150 mM NaCl). The tissue was preincubated in 2% NRS in buffer #1 for 20 min, and then incubated with sheep anti-DIG-AP F(ab), (Catalog number 1093–274, Boehringer-Mannheim) diluted 1: 500 in buffer #1, for 1 hr. The slides were rinsed one time in buffer #1, followed by a 10 min rinse in buffer #2 (100 mM Tris–Cl, 100 mM NaCl, 50 mM $MgCl_2$ [pH 9.5]). Lastly, the substrate solution containing 450 μg/ml of nitro blue tetrazolium salt, B-M, and 175 μg/ml of 5-bromo-4-chloro-3-indolyl phosphate toludium salt, B-M, and 1.25 mM levamisole (Vector Labs) in buffer #2 was added to the tissue, and incubated for 24–48 hr in the dark at 4°C. After sufficient substrate development, the slides were washed extensively in Tris–EDTA (10 mM Tris–HCl [pH 8.0], 1 mM EDTA [pH 8.0]) and mounted with Aquamount (Lerner Laboratories, Pittsburgh, Pennsylvania).

Acknowledgments

We wish to thank Dr. R. Pat Bucy (University of Alabama) for kindly providing the Cμ plasmid, and Dr. Mary Williams (Boston University) for generous use of her cryostat. This work was supported by United States Public Health Service grants T32-CA64070–01 (B. A. J.), AI32531 (A. K. A.), AR35230 (A. M.-R.), AI32137–04 (J. E.), and the Pew Charitable Trust (J. E.).

Received July 28, 1995; revised August 28, 1995.

References

Adachi, M., Watanabe-Fukunaga, R., and Nagata, S. (1993). Aberrant transcription caused by the insertion of an early transposable element in an intron of the Fas antigen gene of *lpr* mice. Proc. Natl. Acad. Sci. USA *90*,1756–1760.

Berek, C., Berger, A., and Apel, M. (1991). Maturation of the immune response in germinal centers. Cell *67*, 1121–1129.

Bloom, D.D., Davignon, J.-L., Retter, M.W., Shlomchik, M.J., Pisetsky, D.S., Cohen, P.L., Eisenberg, R.A., and Clarke, S.H. (1993). V region gene analysis of anti-Sm hybridomas from MRL/Mp-*lpr/lpr* mice. J. Immunol. *150*, 1591–1610.

Brunner, T., Mogil, R.J., LaFace, D., Yoo, N.J., Mahboubi, A., Echeverri, F., Martin, S.J., Force, W.R., Lynch, D.H., Ware, C.F., and Green, D.R. (1995). Cell-autonomous Fas (CD95)/Fas-ligand interaction mediates activation-induced apoptosis in T cell hybridomas. Nature *373*, 441–444.

Budd, R.C., Cerottini, J.C., and MacDonald, H.R. (1986). Cultured Lyt-2$^-$L3T4$^-$ T lymphocytes from normal thymus or *lpr* mice express a broad spectrum of cytolytic activity. J. Immunol. *137*, 3734–3741.

Chu, Y.W., Marin, E., Fuleihan, R., Ramesh, N., Rosen, F.S., and Geha, R. S. (1995). Somatic mutation of human immunoglobulin V genes in the X-linked hyperIgM syndrome. J. Clin. Invest. *95*, 1389–1393.

Cohen, P.L., and Eisenberg, R.A. (1991). *Lpr* and *gld*: single gene models of systemic autoimmunity and lymphoproliferative disease. Annu. Rev. Immunol. *9*, 243–269.

Creighton, W.D., Katz, D.H., and Dixon, F.J. (1979). Antigen-specific immunocompetency, B cell function, and regulatory helper and suppressor T cell activities in spontaneously autoimmune mice. J. Immunol. *123*, 2627–2636.

Cyster, J.G., Hartley, S.B., and Goodnow, C.C. (1994). Competition for follicular niches excludes self-reactive cells from the recirculating B-cell repertoire. Nature *371*, 389–395.

Davignon, J.L., Budd, R.C., Ceredig, R., Piguet, P.F., MacDonald, H.R., Cerottini, J.C., Vassalli, P., Izui, S. (1985). Functional analysis of T cell subsets from mice bearing the *lpr* gene. J. Immunol. *135*, 2423–2428.

Dhein, J., Walczak, H., Bäumler, C., Klaus-Michael D., and Krammer, P.H. (1995). Autocrine T cell suicide mediated by APO-1(Fas/CD95). Nature *373*, 438–441.

Eisenberg, R.A., Winfield, J.B., and Cohen, P.L. (1982). Subclass restriction of anti-Sm antibodies in MRL mice. J. Immunol. *129*, 2146–2149.

Erikson, J., Radic, M.Z., Camper, S.A., Hardy, R.R., Carmack, C., and Weigert, M. (1991). Expression of anti-DNA immunoglobulin transgenes in non-autoimmune mice. Nature *349*, 331–334.

Giese, T., and Davidson, W.F. (1994). Chronic treatment of C3H-*lpr/lpr* and C3H-*gld/gld* mice with anti-CD8 monclonal antibody prevents the accumulation of double negative T cells but not autoantibody production. J. Immunol. *152*, 2000–2010.

Giese, T., and Davidson, W.F. (1995). In CD8$^+$ T cell deficient *lpr/lpr* mice, CD4$^+$B220$^+$ and CD4$^+$B220$^-$ T cells replace B220$^+$ double negative T cells as the predominant population in enlarged lymph nodes. J. Immunol. *154*, 4986–4995.

Goding, J.W. (1976). Conjugation of antibodies to fluorochromes: modifications to standard methods. J. Immunol. Meth. *13*, 215–226.

Hammond, D.M., Nagarkatti, P.S., Goté, L.R., Seth, A., Hassuneh, M.R., and Nagarkatti, M. (1993). Double-negative T cells from MRL-*lpr/lpr* mice mediate cytolytic activity when triggered through adhesion molecules and constitutively express perforin gene. J. Exp. Med. *178*, 2225–2230.

Heitzman, H., and Richards, F.M. (1974). Use of the avidin–biotin complex for specific staining of biological membranes in electronmicroscopy. Proc. Natl. Acad. Sci. USA *71*, 3537–3541.

Itoh, N., Yonehara, S., Ishii, A., Yonehara, M., Mizushima, S.-I., Sameshima, M., Hase, A., Seto, Y., and Nagata, S. (1991). The polypeptide encoded by the cDNA for human cell surface antigen Fas can mediate apoptosis. Cell *66*, 233–243.

Jacob J., Kassir, R., and Kelsoe, G. (1991a). In situ studies of the primary immune response to (4-hydroxy-3-nitrophenyl)acetyl. I. The architecture and dynamics of responding cells populations. J. Exp. Med. *173*, 1165–1175.

Jacob, J., Kelsoe, G., Rajewsky, K., and Weiss, U. (1991b). Intraclonal generation of antibody mutants in germinal centres. Nature *354*, 389–392.

Jacobson, B.A., Sharon, J., Shan, H., Shlomchik, M., Weigert, M.G., and Marshak-Rothstein, A. (1994). An isotype switched and somatically mutated rheumatoid factor clone isolated from a MRL-*lpr/lpr* mouse exhibits limited intraclonal affinity maturation. J. Immunol. *152*, 4489–4499.

Ju, S.-T., Panka, D.J., Cui, H., Ettinger, R., El-Khatib, M.R., Sherr, D.H., Stanger, B.Z., and Marshak-Rothstein, A. (1995). Fas (CD95)/FasL interactions required for programmed cell death after T cell activation. Nature *373*, 444–448.

Klinman, D. M. (1990). Polyclonal B cell activation in lupus-prone mice precedes and predicts the development of autoimmune disease. J. Clin. Invest. *86*, 1249–1254.

Lieberum, B., and Hartmann, K.-U. (1988). Successive changes of the cellular composition in lymphoid organs of MRL–Mp/*lpr–lpr* mice during the development of lymphoproliferative disease as investigated in cryosections. Clin. Immmunol. Immunopath. *46*, 421–431.

Liu, Y.-J., Zhang, J., Lane, P.J.L., Chan, E.Y.-T., and MacLennan, I.C.M. (1991). Sites of specific B cell activation in primary and secondary responses to T cell dependent and T cell independent antigens. Eur. J. Immunol. *21*, 2951–2962.

MacLennan, I.C.M., Liu, Y.-J., Oldfield, S., Zhang, J., and Lane, P.J.L. (1990). The evolution of B-cell clones. Curr. Topics Microbiol. Immunol. *159*, 37–63.

McHeyzer-Williams, M.G., McLean, M.J., Lalor, P.A., and Nossal, G.J.V. (1993). Antigen-driven B cell differentiation in vivo. J. Exp. Med. *178*, 295–307.

Mitchell, J. (1973). Lymphocyte circulation in the spleen: marginal zone bridging channels and their possible role in cell traffic. Immunology *24*, 93–107.

Mixter, P.F., Russell, J.Q., Durie, F.H., and Budd, R.C. (1995). Decreased CD4$^-$CD8$^-$ TCR-αβ$^+$ cells in *lpr/lpr* mice lacking β2-microglobulin. J. Immunol. *154*, 2063–2074.

Morse, H.C., Davidson, W.F., Yetter, R.A., Murphy, E.D., and Roths, J.B. (1982). Abnormalities induced by the mutant gene *lpr*: expansion of a unique lymphocyte subset. J. Immunol. *129*, 2612–2615.

Mountz, J.D., Smith, H.R., Wilder, R.L., Reeves, J.P., and Steinberg, A.D. (1987). CS-A therapy in MRL-*lpr/lpr* mice: amelioration of immu-

nopathology despite autoantibody production. J. Immunol. *183*, 157–163.

Nemazee, D., Guiet, C., Buerki, K., and Marshak-Rothstein, A. (1991). B lymphocytes from the autoimmune-prone mouse strain MRL/*lpr* manifest an intrinsic defect in tetraparental MRL/*lpr* ↔ DBA/2 chimeras. J. Immunol. *147*, 2536–2539.

Park, C.L., Balderas, T.S., Fieser, T.M., Slack, J.H., Prud'homme, G.J., Dixon, F.J., and Theofilopoulos, A.N. (1983). Isotypic profiles and other fine characteristics of immune responses to exogenous thymus-dependent and -independent antigens by mice with lupus syndromes. J. Immunol. *130*, 2161–2167.

Perkins, D.L., Glaser, R.M., Mahon, C.A., Michaelson, J., and Marshak-Rothstein, A. (1990). Evidence for an intrinsic B cell defect in *lpr*/*lpr* mice apparent in neonatal chimeras. J. Immunol. *145*, 549–555.

Prud'homme, G.J., Park, C.L., Fieser, T.M., Kofler, R.,. Dixon, F.J., and Theofilopoulos, A.N. (1983). Identification of a B cell differentiation factor(s) spontaneously produced by proliferating T cells in murine lupus strains of the *lpr*/*lpr* genotype. J. Exp. Med. *157*, 730–742.

Radic, M.Z., Mascelli, M.A., Erikson, J., Shan, H., and Weigert, M. (1991). Ig H and L chain contributions to autoimmune specificities. J. Immunol. *146*, 176–182.

Rathmell, J.C., and Goodnow, C.C. (1994). Effects of the *lpr* mutation on elimination and inactivation of self-reactive B cells. J. Immunol. *153*, 2831–2842.

Rathmell, J.C., Cooke, M.P., Ho, W.Y., Grein, J., Townsend, S.E., Davis, M.M., and Goodnow, C.C. (1995). CD95 (Fas)-dependent elimination of self-reactive B cells upon interaction with $CD4^+$ T cells. Nature *376*, 181–184.

Roark, J.H., Kuntz, C.L., Nguyen, K.-A., Caton, A.J., and Erikson, J. (1995). Breakdown of B cell tolerance in a mouse model of sytemic lupus erythematosus. J. Exp. Med. *181*, 1157–1167.

Rothstein, T.L., Wang, J.K.M., Panka, D.J., Foote, L.C., Wang, Z., Stanger, B., Cui, H., Ju, S.-T., and Marshak-Rothstein, A. (1995). Protection against Fas-dependent Th1-mediated apoptosis by antigen receptor engagement in B cells. Nature *374*, 163–165.

Rubin, R.L., Tang, F.-L., Chan, E.K.L., Pollard, K.M., Tsay, G., and Tan, E.M. (1986). IgG subclasses of autoantibodies in systemic lupus erythematosus, Sjögren's syndrome, and drug-induced autoimmunity. J. Immunol. *137*, 2528–2534.

Shlomchik, M.J., Marshak-Rothstein, A., Wolfowicz, C.B., Rothstein, T.L., and Weigert, M.G. (1987). The role of clonal selection and somatic mutation in autoimmunity. Nature *328*, 805–811.

Shlomchik, M., Mascelli, M., Shan, H., Radic, M.Z., Pisetsky, D., Marshak-Rothstein, A., and Weigert, M. (1990). Anti-DNA antibodies from autoimmune mice arise by clonal expansion and somatic mutation. J. Exp. Med. *171*, 265–292.

Shokat, K.M., and Goodnow, C.C. (1995). Antigen-induced B-cell death and elimination during germinal-centre immune response. Nature *375*, 334–338.

Slack, J.H., LeMing, H., Barkley, J., Fulton, R.J., D'Hoostelaere, L., Robinson, A., and Dixon, F.J. (1984). Isotypes of spontaneous and mitogen-induced autoantibodies in SLE-prone mice. J. Immunol. *132*, 1271–1275.

Sobel, E.S., Katagiri, T., Katagiri, K., Morris, S.C., Cohen, P.L., and Eisenberg, R.A. (1991). An intrinsic B cell defect is required for the production of autoantibodies in the *lpr* model of systemic autoimmunity. J. Exp. Med. *173*, 1441–1449.

Takahasi, T., Tanaka, M., Brannan, C.I., Jenkins, N.A., Copeland, N.G., Suda, T., and Nagata, S. (1994). Generalized lymphoproliferative disease in mice caused by a point mutation in the Fas ligand. Cell *76*, 969–976.

Theofilopoulos, A.N., and Dixon, F.J. (1985). Murine models of systemic lupus erythematosus. Adv. Immunol. *37*, 269–390.

Trauth, B.C., Klas, C., Peters, A.M., Matzku, S., Moler, P., Falk, W., Debatin, K.M., and Krammer, P. (1989). Monoclonal antibody–mediated tumor regression by induction of apoptosis. Science *245*, 301–305.

Unkeless, J.C., and Eisen, H.N. (1975). Binding of monomeric immunoglobulins to Fc receptors of mouse macrophages. J. Exp. Med. *142*, 1520–1533.

Van den Eertwegh, A.J.M., Boersma, W.J.A., and Claassen, E. (1992). Immunological functions and in vivo cell–cell interactions of T cells in the spleen. Crit. Rev. Immunol. *11*, 337–380.

Van den Eertwegh, A.J.M., Noelle, R.J., Roy, M., Shepard, D.M., Aruffo, A., Ledbetter, J.A., Boersma, W.J.A., and Claassen, E. (1993). In vivo CD40–gp39 interactions are essential for thymus-dependent humoral immunity. I. In vivo expression of CD40 ligand, cytokines and antibody production delineates sites of cognate T–B cell interactions. J. Exp. Med. *178*, 1555–1565.

Van Ewijk, W., Rozing, J., Brons, N.H.C., and Klepper, D. (1977). Cellular events during the primary immune response in the spleen: a fluorescent-, light-, and electronmicroscopic study in germ free mice. Cell Tissue Res. *183*, 471–489.

Van Rooijen, N., Claassen, E., and Eikelenboom, P. (1986). Is there a single differentiation pathway for all antibody-forming cells in the spleen. Immunol. Today *7*, 193–195.

Very, D.L., Panka, D.J., Weissman, D., Wysocki, L., Manser, T., and Marshak-Rothstein, A. (1993). Lack of connectivity between the induced and autoimmune repertoires of *lpr*/*lpr* mice. Immunology *80*, 518–526.

Wallach, J. (1992). Interpretation of Diagnostic Tests: A Synopsis of Laboratory Medicine. (Boston: Little, Brown and Company), pp. 694–698.

Watanabe-Fukunaga, R., Brannan, C.I., Itoh, N., Yonehara, S., Copeland, N.G., Jenkins, N.A., and Nagata, S. (1992a). The cDNA structure, expression, and chromosomal assignment of the mouse Fas antigen. J. Immunol. *148*, 1274–1279.

Watanabe-Fukunaga, R., Brannan, C.I., Copeland, N.G., Jenkins, N.A., and Nagata, S. (1992b). Lymphoproliferative disorder in mice explained by defects in the antigen that mediates apoptosis. Nature. *356*, 314–317.

Wolfowicz, C.B., Sakorafas, P., Rothstein, T.L., and Marshak-Rothstein, A. (1988). Oligoclonality of rheumatoid factors arising spontaneously in *lpr*/*lpr* mice. *Clin. Immunol. Immunopathol. 46*, 382–395.

Yonehara, S., Ishii, A., and Yonehara, M. (1989). A cell-killing monoclonal antibody (anti-Fas) to a cell surface antigen co-downregulated with the receptor of tumor necrosis factor. J. Exp. Med. *169*, 1747–1756.